

Kinetic modelling of epitaxial film growth with up- and downward step barriers

F.F. Leal^{1,2}, T. J. Oliveira¹ and S. C. Ferreira^{1‡}

¹Departamento de Física - Universidade Federal de Viçosa, 36571-000, Viçosa, Minas Gerais, Brazil

²Instituto Federal de Ciência, Educação e Tecnologia - Campus Itaperuna, Rodovia BR 356 - KM 03, 28300-000, Itaperuna, Rio de Janeiro, Brazil.

E-mail: ffeal@iff.edu.br, silviojr@ufv.br, tiago@ufv.br

Abstract. The formation of three-dimensional structures during the epitaxial growth of films is associated to the reflection of diffusing particles in descending terraces due to the presence of the so-called Ehrlich-Schwoebel (ES) barrier. We generalize this concept in a solid-on-solid growth model, in which a barrier dependent on the particle coordination (number of lateral bonds) exists whenever the particle performs an interlayer diffusion. The rules do not distinguish explicitly if the particle is executing a descending or an ascending interlayer diffusion. We show that the usual model, with a step barrier in descending steps, produces spurious, columnar, and highly unstable morphologies if the growth temperature is varied in a usual range of mound formation experiments. Our model generates well-behaved mounded morphologies for the same ES barriers that produce anomalous morphologies in the standard model. Moreover, mounds are also obtained when the step barrier has an equal value for all particles independently if they are free or bonded. Kinetic roughening is observed at long times, when the surface roughness w and the characteristic length ξ scale as $w \sim t^\beta$ and $\xi \sim t^\zeta$ where $\beta \approx 0.31$ and $\zeta \approx 0.22$, independently of the growth temperature.

PACS numbers: 05.70.Ln, 89.75.Da, 89.75.Hc, 05.70.Jk

Submitted to: *J. Stat. Mech.: Theor. Exp.*

1. Introduction

Since epitaxial techniques became available, a large number of experimental works reporting on the production of films with three-dimensional patterned structures, called generically of mounds, as well as the analytical and computational modelling devoted to explain these patterns have been found in literature (see Ref. [1] for a review). Mounds have been observed during the growth of a wide diversity of films, ranging from metals [2, 3, 4] to inorganic [5, 6] and organic [7, 8] semiconductor materials. The morphological properties, one of the most important features in film production,

‡ On leave at Departament de Física i Enginyeria Nuclear, Universitat Politècnica de Catalunya, Spain.

depend of distinct physical mechanisms as diffusion rate [9, 1], deposition rate [10], growth temperature [11, 6], deposition shadowing [12], among others.

During the film production, the surface may follow distinct growth regimes [1]. The so-called kinetic roughening, where the surface dynamics is described by scale invariance, has significant interest. The power law behaviours of the surface rms width $w \sim t^\beta$ and the characteristic correlation length $\xi \sim t^\zeta$ are the basic scaling laws involved in the kinetic roughening, defining the growth and coarsening exponents, respectively. There is a third, not independent exponent related to the scaling of the global surface fluctuations, the roughness exponent $\alpha = \beta/\zeta$ [13]. Two scaling regimes are of special interest in mound formation: The first one involves slope selection [14, 15, 16], where the ratio between the characteristic length and the surface width approaches a constant value. This condition is satisfied for $\beta = \zeta$. The second one is the super-roughness scaling regime [17, 13], characterized by $\alpha > 1$. The latter implies that the surface is locally smooth, having different scaling exponents for global and local fluctuations [17].

The mound formation during the epitaxial growth is frequently associated to the reflection of particles (atoms or molecules) in descending terraces due to presence of the so-called Ehrlich-Schwoebel (ES) barrier [1]. The explanation for this step barrier is founded in the experimental observation that particles are reflected backwards in the terrace edges more frequently than move to a lower layer [18, 19]. Although other mechanisms, as short-range attraction towards ascending steps [20] and fast edge diffusion [21, 22, 23] can lead to mound formation, they are weaker than the ES barrier.

Kinetic Monte Carlo (KMC) is a standard simulation method for atomistic modelling of epitaxial growth. The basic idea was formerly introduced by Clarke and Vvedensky [24, 25] and generalized in many other frameworks [1, 9]. In the Clarke-Vvedensky model, diffusion is a thermally activated process described by an Arrhenius law $D \sim \exp(-E/k_B T)$ [9], where E is a diffusion activation energy, T the temperature and k_B the Boltzmann constant. The ES barrier is usually modelled with an additional energy barrier E_b to particles moving downwards in the edge of a terrace [1]. In a simplified picture, E_b is the additional energy needed when a particle crosses a step edge. Therefore, a step barrier must also exist for particles performing upward diffusion (see Fig. 1). However, the ES barrier is generally considered only for particles diffusing from an upper to a lower terrace and barriers for ascending steps were considered in a limited number of models. Šmilauer and Vvedensky [14] proposed a step barrier proportional to the difference between next-nearest neighbour (NNN) bonds before and after the particle hop only if the number of NNN bonds decreases after the hop, independently if the adatom performs an up- or downward diffusion. Recently, a model with a barrier dependent on the step height was investigated [26]. Besides the barrier in descending steps, this model also assumes an ascending barrier for multilayer steps. However, the barrier in monolayers was implemented as usual and the model is not fully symmetric in to relation down- and upward step diffusion. Barriers in ascending steps were also considered in the limited mobility model of Wolf-Villain [27], where probabilities of moving to lower or upper terraces after a deposition step were introduced. Mound

formation is obtained when the probability of upward diffusion is larger than downward diffusion.

In the present work, we revisit the effects of ES barriers in KMC simulations by comparing the standard model, having a barrier only in descending steps, with the case where a barrier for upward diffusion is also activated. Moreover, we consider different barriers depending if the particle has or not lateral bonds. The model allows to investigate the interesting symmetric case where bonded and free (with no lateral bonds) particles undergo the same barrier. We show that the standard bond counting model produces unrealistic columnar mounds when the diffusion of particles with lateral bonds cannot be neglected. This feature limits the applicability of this model to a short range of temperature. On the other hand, the model with a bond dependent step barrier produces well-behaved mounded surfaces in a wide range of temperature, consistent with typical experimental conditions.

We have organized the paper as follows. In Sec. 2 we present the models and KMC simulation strategies. Comparison between a barrier exclusively to downward diffusion and the bond dependent step barrier is done in Sec. 3. Further analyses of our model, including the symmetric case, are presented and discussed in Sec. 4. We summarize our results and conclusions in Sec. 5.

2. Kinetic Monte Carlo model

We model homoepitaxy on a substrate at a temperature T represented by a triangular lattice with periodic boundary conditions. Particles are deposited at a constant rate F under the solid-on-solid restriction, implying that voids and overhangs are absent. A deposition event consists in increasing the height by $h_j \rightarrow h_j + 1$, where h_j is the number of particles deposited in the site j . The choice of the deposition site j is done in two steps: Firstly a site is chosen at random, and secondly a new particle is deposited in the most energetically favourable (largest bond number) site among the chosen one and its nearest neighbours (NN). This transient mobility is justifiable if we consider that the particle arrives at the substrate with a kinetic energy higher than the typical activation energy in the substrate ($k_B T$). This deposition rule corresponds to the classical Wolf-Villain (WV) model [28]. The transient mobility in the deposition rule plays an important role in the surface morphology at low temperatures, as we will show in Sec. 4. It is important to mention that a transient mobility was used in previous models of epitaxial growth with thermally activated diffusion [1, 14].

Intra and interlayer thermally activated diffusion are allowed for any surface particle. Diffusion happens between NN sites and depends on the initial and final position of the particle. The diffusion rate from site j to a neighbour j' is given by the Arrhenius law

$$D(j, j'; T) = \nu \exp \left[-\frac{E(j, j')}{k_B T} \right], \quad (1)$$

where ν is an attempt frequency and E the diffusion activation energy given by

$$E(j, j') = E_0 + n_j E_N + E_b(j, j'). \quad (2)$$

The energy E_0 represents the interaction with the substrate and/or bulk of the film, E_N is the contribution of each one of n_j lateral bonds, and E_b is the step barrier present for interlayer diffusion. Apart of the step-edge barrier, the model is equivalent to the thermal activation model proposed by Šmilauer and Vvedenski [14]. Algorithmically, the step barrier is present only if $\Delta h(j, j') \neq 0$, where $\Delta h(j, j') \equiv h_{j'} + 1 - h_j$.

Apart from the details of the barrier rules, which are described below, the kinetic Monte Carlo simulations are implemented as follows. A particle is deposited and then N diffusion attempts are sequentially implemented. In a diffusion attempt, a particle of the surface is selected at random and its diffusion is implemented accordingly to the ratio D/F given by Eq. (1). The diffusion is efficiently implemented by keeping updated lists containing the positions of the particles with the same number of lateral bonds. Let ρ_n , $n = 0, 1, \dots, 6$ be the fraction of particles with n lateral bonds. Between two deposition events, the average number of diffusion attempts of the particles having n bonds is $N_n = \rho_n D(n; T)/F$ where

$$D(n; T) = \nu \exp \left(-\frac{E_0 + n E_N}{k_B T} \right) \quad (3)$$

is the diffusion rate excluding the step barrier contribution. In the implementation, we sequentially choose $N = \sum_{n=0}^6 N_n \dagger$ particles, with the coordination number obeying the ratio $N_0 : N_1 : \dots : N_6$. For each selected particle (site j), a neighbour (site j') is chosen with equal chance and the particle hops to this site with probability

$$P_h(j, j'; T) = \exp \left[-\frac{E_b(j, j')}{k_B T} \right], \quad (4)$$

which includes the effect of the step barrier. With the complementary probability the particle stays in the same site. The process is repeated until the runs of N diffusion attempts are finished and a new particle deposited.

In the present work, we are interested in the effect of an uphill in addition to the usual downhill step-edge barrier. Figure 1 shows some important situations involving interlayer diffusion. Let us firstly consider the particles A and C lying in monosteps. In both cases, it is intuitive that staying in the same layer is favoured since, otherwise, the particle has to detach and rebind in an adjacent layer. So, an additional step barrier (not necessarily equal) must be present in both configurations. The kink particle B , however, should diffuse up- or downwards with equal chance due to the local symmetry of this configuration. In a simple description, particles A and B may be subject to a similar step barrier that may possibly be different from the barrier for particle C .

Our model has descending and ascending interlayer diffusions that depend if the particles are bonded or not. By simplicity, we assume two kind of step barriers: E_{b0}

\dagger More precisely, the number of attempts is increased by 1 with probability $N - \bar{N}$, were \bar{N} is truncation to the integer part of N

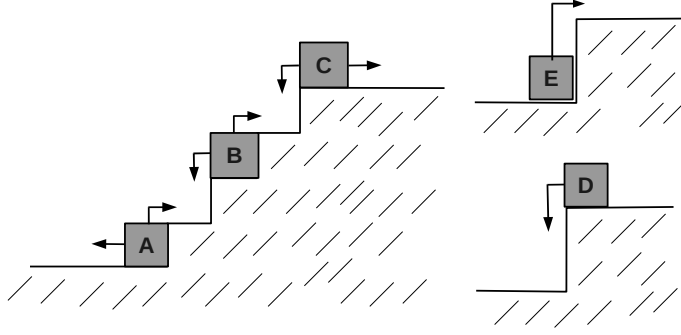


Figure 1. Illustration of important situations involving interlayer diffusion: Diffusion through monolayer (left) and multilayer (right) steps. Both, particles D and E have to overcome a barrier when moving through the steps.

for free particles ($n = 0$) and E_{bn} for bonded particles ($n \geq 1$). Notice that rules do not concern explicitly if the particles are moving down- or upwardly, but, free particles will never be in an ascending step since this configuration requires $n \geq 1$. In principle, configurations D and E are apparently equivalent but the situation is much more complicated in 2+1 dimensions due to the bonds not shown in an 1+1 representation. However, it is clear that a step barrier must exist for both particles and our model is, therefore, an improvement for these configurations. Actually, as shown in Ref. [26], although the presence of a barrier in a multilayer step is important, the details of the barrier dependence with the step height do not alter significantly the final surface morphology. We refer to our rules as BDSB (bond dependent step barrier) while the standard model we call of DSB (downward step barrier).

3. Results: BDSB versus DSB models

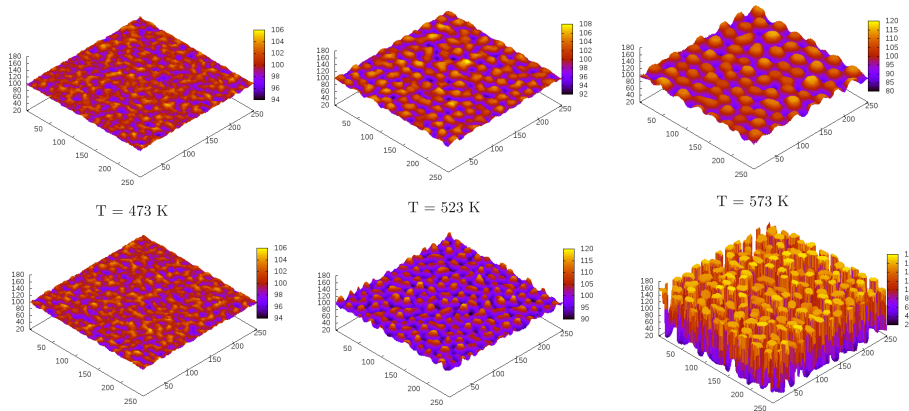


Figure 2. Surface morphologies for the BDSB (top) and the DSB (bottom) models for distinct temperatures after a deposition of 100 ML. The step barriers in the BDSB model are $E_{bn} = 0$ and $E_{b0} = 0.05$ eV while the barrier in the DSB model is $E_b = 0.05$ eV. See supplementary material for surface evolutions.

The KMC simulations were performed with the fixed parameters $E_0 = 1$ eV, $E_N = 0.11$ eV, $F = 1$ monolayers (ML) per second, and $\nu = 10^{13}$ s $^{-1}$. Temperature was varied in the interval $T = 473 - 623$ K corresponding to a range of temperature $\Delta T = 150$ K compatible with several semiconductor and metal film growths [1]. We simulated substrates sizes $L = 256, 512$ and 1024 , and no significant difference was observed in the results. Therefore, except if explicitly mentioned, the results correspond to $L = 512$.

In order to analyse the effects of the step barrier for kink particles, we compare the DSB and BDSB models using a null barrier for bonded particles ($E_{bn} = 0$). In this case, BDSB includes an ES barrier only for free particles in descending steps while in DSB model the ES barrier is always present in downward movements. Figure 2 shows the surface morphologies for three temperatures after a deposition of 100 monolayers. A fixed step barrier of 0.05 eV is used for free particles in BDSB model and for downward diffusion in DSB model. Both models exhibit mounded morphologies, qualitatively similar at low temperatures (see $T = 473$ K, for example). However, when temperature is increased, the surfaces of DSB model become anomalously mounded, with unrealistic columnar structures and huge steps while regular mounded morphologies are observed for BDSB. If the deposition time is increased, the surface for $T = 523$ K also develops columnar mounds in DSB model, but does not for BDSB, as can be seen in the videos 1 and 2 of the supplementary material. Increasing step barrier, representing more realistic values in many systems, strongly enhances the anomaly in the DSB whereas BDSB remains well-behaved (data not shown).

The DSB unrealistic behaviour at high temperatures has a simple explanation formerly realized by Villain [29]: For a particle in a descending step (particle C, Fig. 1), the chances of attachment in an ascending step or of a new terrace nucleation in the same layer are greater than the chances of attachment in the subjacent step due to ES barrier. However, at high temperatures, when a particle in an ascending step (particle A, Fig. 1) has a non-negligible mobility, the detachment and climbing chances are equal and the asymmetry of the rule for kink particles (particle B, Fig. 1) produces a large destabilizing uphill current. This result shows that the step barrier in the kink particles plays a central role in the determination of the mound morphology.

A basic quantity used to characterize the surface morphology is the height-height correlation function defined as [21, 22]

$$\Gamma(\mathbf{r}) = \langle h(\mathbf{x})h(\mathbf{x} + \mathbf{r}) \rangle_{\mathbf{x}}, \quad (5)$$

where $h(\mathbf{x})$ is the surface in the mean height reference and $\langle \dots \rangle_{\mathbf{x}}$ is the average over the surface. The interface width (rms roughness) w is given by $\sqrt{\Gamma(0)}$ and the first maximum of $\Gamma(r)$ measures an average distance between mounds δ . Figure 3(a) shows the height-height correlation function against distance for systems at different temperatures. The curves were rescaled by $\Gamma(0)$ to improve visibility. The oscillating correlation function is the hallmark of mounded surfaces [1, 21]. Figure 3(b) shows the surface width and mound separation against temperature for both models. The interface width grows

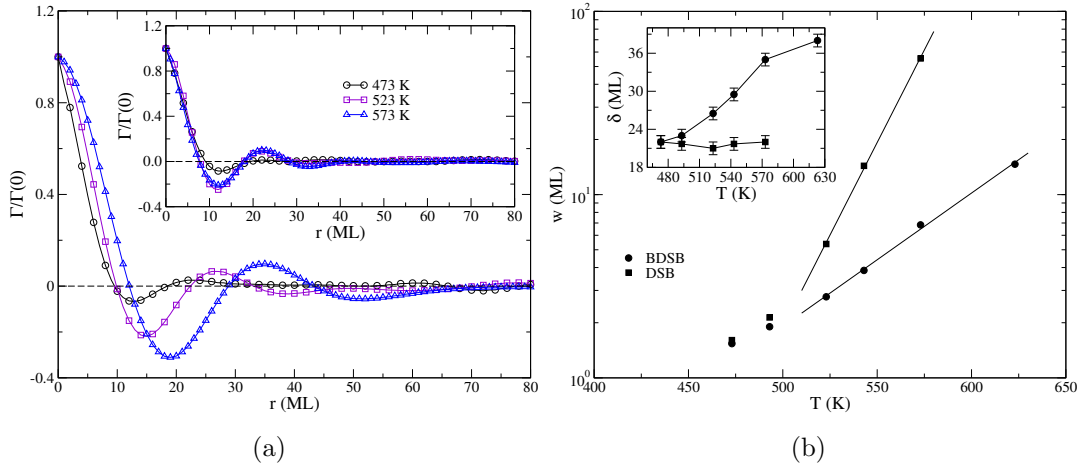


Figure 3. Surface morphological characterization for BDSB and DSB models. (a) Height-height correlation function after the deposition of 100 ML at distinct temperatures. Results for BDSB and DSB models are shown in the main plot and inset, respectively. (b) Interface width (main plot) and characteristic mound separation (inset) against temperature. The fixed parameters are the same used in Fig. 2.

exponentially with temperature in both cases meaning a temperature driven instability, but the DSB produces anomalously huge surface widths in the investigated temperature interval. The characteristic mound distance is closely constant for DSB and grows monotonically with temperature for BDSB, as shown in the inset of Fig. 3(b).

It is important noticing that DSB model produces a closely constant mound separation and a fast increase of the surface width with temperature. Morphologically, we have a strong increase of the mound heights and grooves. At higher temperatures (not shown), the uphill currents are so intense that parts of the initial substrate remain uncovered, and highly columnar structures are completely formed upon the template of sub-monolayer islands.

The growth of three-dimensional structures involves a complex relation between the down- and upward fluxes through the steps in addition to the adsorption and nucleation mechanisms. We quantify the net flux through steps using an out-of-plane current defined by

$$J_z = \frac{1}{2L^2} \sum_j D(n_j; T) \frac{1}{q} \sum_{j' \in \mathcal{V}(j)} \Theta[\Delta(j, j')] P_h(j, j'; T), \quad (6)$$

in which the sum over j runs over all sites while the sum over j' runs over all q nearest neighbours of j . The factor $1/2$ accounts for the double counting of bonds (j, j') . The factor $D(n_j; T)$ is given by Eq. (3), $P_h(j, j'; T)$ by Eq. (4), and $\Theta(x)$ returns the sign of x and $\Theta(0) = 0$. This quantity is the average interlayer diffusion rate per site since the intralayer diffusion is not counted. In order to reduce statistical fluctuations, the current at a time t is the average over a short interval δt around t . The currents for the BDSB and DSB models are compared in Fig. 4. For low temperatures, the currents show a downward (negative) flux in both models that is attenuated in the DSB due to

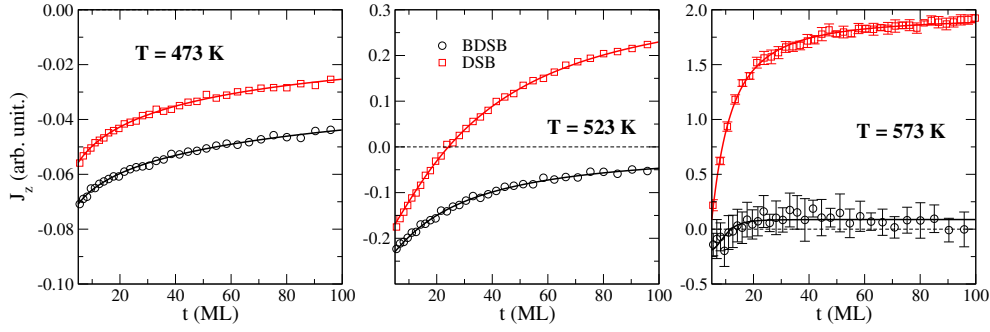


Figure 4. Out-of-plane currents against time for BDSB and DSB models at distinct temperatures. Step barriers are the same used in simulations shown in Fig. 2. Symbols represent simulations and solid line sigmoid regressions as guides to the eyes. The data correspond to averages over 50 samples and the error bars smaller than symbols were omitted.

the absence of barrier to upward diffusion. The flux tends monotonically and slowly to zero. Apart of a short initial transient, the data is very well fitted by a Hill function

$$J_z = -j_0 + j_0 \frac{t^\eta}{A + t^\eta} \quad (7)$$

with exponents $\eta \approx 0.34$ and $\eta \approx 0.48$ for BDSB and DSB, respectively. For intermediate temperatures, the BDSB current also grows monotonically to a zero flux while a very large positive current is observed in DSB. For high temperatures, both models have positive currents, but the currents in BDSB are much smaller than in DSB.

Slope selection is an important feature in mound formation [14, 15, 16], where the ratio between characteristic width and height tends to a constant value at long times. In terms of continuous equation approaches, the slope selection involves a balance between up- and downhill currents [15, 16] that is strongly violated in DSB model at intermediate and high temperatures, as shown in Fig. 4. The current in the BDSB model at low and intermediate temperatures, on other hand, grows monotonically to a balance steady-state implying slope selection. The decaying and positive current observed at high temperatures also states slope selection for $t \rightarrow \infty$, but the time required to observe it is very large due to a very slow decay (Fig. 5(b) shows a quantitative analysis for other parameters). The absence of a characteristic slope in DSB model is also evident in Fig. 2 due to the anomalous columnar morphology. Video 2 of the Supplementary Material further illustrates the absence of slope selection in DSB model.

4. KMC simulations of the BDSB model

Now, we concentrate in the effects of the uphill step barrier. The imbalance that promotes the uphill destabilizing current and mound formation can be controlled with the step barriers for free and bonded particles. Fig. 5(a) shows the surface width and characteristic length for the interesting symmetric case, in which the barrier is the same for all particles, $E_{b0} = E_{bn} = 0.06$ eV. The interface width is strongly reduced

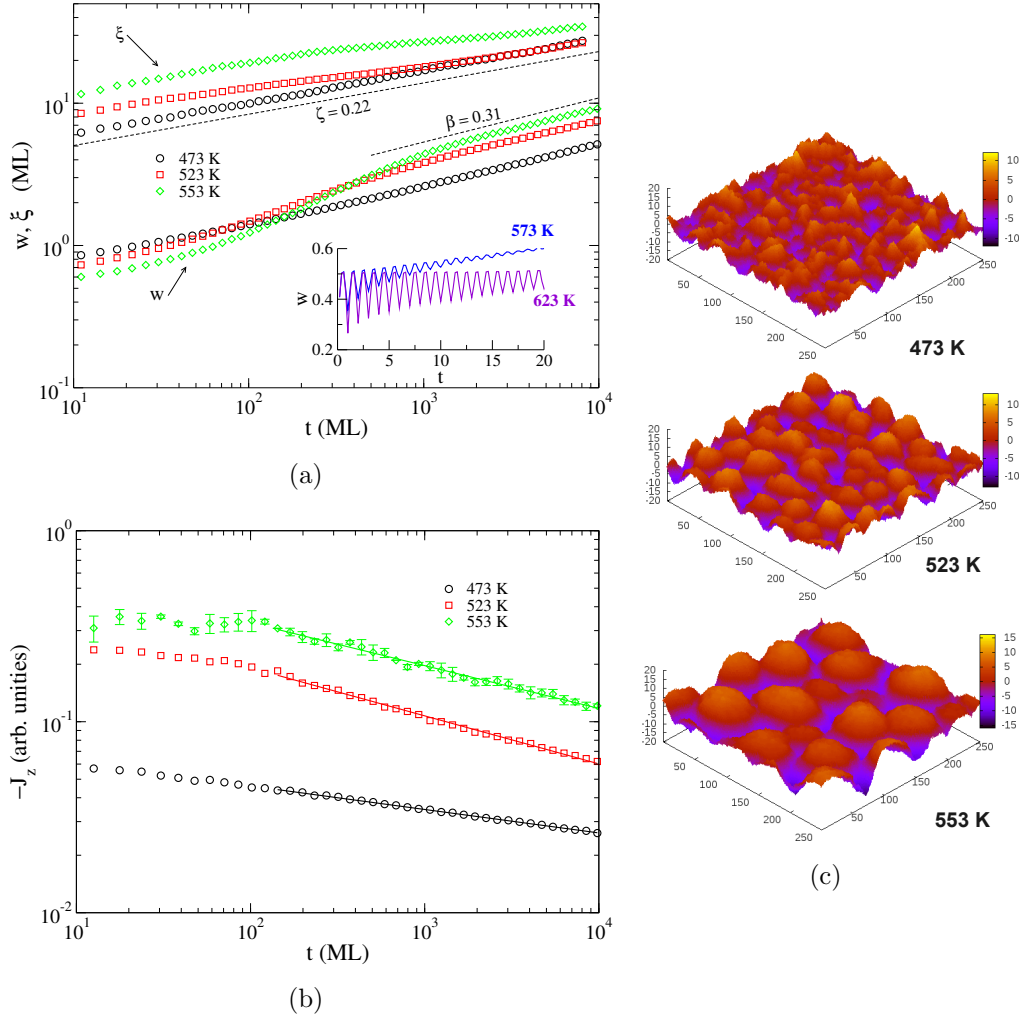


Figure 5. Surface dynamics for symmetric BDSB model with $E_{b0} = E_{bn} = 0.06$ eV. (a) Interface width and characteristic length against time. Inset shows the interface width at short times. (b) Out-of plane current against time. Solid lines are power regressions and error bars smaller than symbols were omitted. (c) Surface morphologies after deposition of 10^3 ML.

if compared with the asymmetric barrier case shown in Figs. 2 and 3. Therefore, an important role of the uphill step barrier is the stabilization and smoothing of surfaces implying reduction of the three-dimensional structure amplitudes.

At high temperatures, the interface width presents an initial oscillating behaviour of a layer-by-layer growth regime as shown in the inset of Fig. 5(a). At longer times, the layer-by-layer growth is replaced by a kinetic roughening featured by asymptotic power laws $w \sim t^\beta$ and $\xi \sim t^\zeta$, with exponents $\beta \approx 0.31$ and $\zeta = 0.22$. Here, the characteristic length is defined as the first zero of height-height correlation function [21, 22]. The coarsening exponent obtained in our simulations is close to that observed in a model with a barrier dependent on the next nearest neighbours [14]. Our simulations point out that the exponents are independent of temperature and barrier strength, even though the asymptotic scaling regime of the characteristic length was not reached in our simulations

at high temperatures. The layer-by-layer phase becomes longer for higher temperatures since, in these situations, the particles have enough energy to overcome the edge barrier and to bind to highly coordinated sites at the adjacent layers. The kinetic roughening was formerly explained by Villain [29] in terms of the particle edge reflection caused by the ES barrier to the downward movement, as discussed in Sec. 3. For the symmetric barrier model, the origin of the kinetic roughening is similar but the imbalance between downward and upward currents is additionally because of particles in ascending steps (bonded by definition) are, in an average, less diffusing than those in descending ones. Notice that symmetric barriers hinder mound formation in the WV model in $d = 1 + 1$ dimensions [27]. Mound formation was observed in the WV model in $d = 2 + 1$ without step-barrier, but the artefact of noise reduction was necessary to overcome the very slow crossover to the asymptotic limit [22].

Figure 5(a) also shows a re-entrant behaviour of the interface width as function of temperature for intermediate growth times $t \simeq 100 - 300$ ML. Re-entrant behaviours, which mean an interface width firstly increasing and then decreasing with temperature (no monotonic dependence), were reported in a classical experiment [30] and the corresponding kinetic modelling [31, 32] of the growth of Ag/Ag(100), among other systems [1]. While specific models were devoted to describe this complex behaviour [1, 31, 32], it has appeared spontaneously in our simulations during the crossover between layer-by-layer and kinetic roughening growth regimes.

Interlayer currents against time for the symmetric barrier simulations are shown in Fig. 5(b). The results differ from the asymmetric barrier model since the current is always negative and approaches zero as a power law $J_z \sim -t^{-\eta}$ with exponents $\eta = 0.1 - 0.25$. This algebraic decay means that the balance between down- and uphill diffusion, theoretically required for slope selection, will be reached only at infinite times when the interface widths are already saturated. In fact, the growth and coarsening exponents obtained in our simulations obey the relation $\beta > \zeta$ that implies an aspect ratio of the mounds (height/width) increasing with time and, consequently, no slope selection is strictly observed. A growth exponent greater than the coarsening exponents also means that the surface is described by the so-called super-roughness scaling regime [13] for which the roughness exponent $\alpha = \beta/\zeta > 1$. Generic scaling theory states that $\alpha > 1$ implies in locally smooth surface where the interface width in a scale of size ϵ scales linearly as $w \sim \epsilon$ [13].

Surface morphologies obtained with symmetric barriers at distinct temperatures are shown in Figure 5(c), where one can clearly see three-dimensional structures and mounds for the investigated temperature range. The mound shape is approximately pyramidal for the lower temperature ($T = 473$ K) and becomes dome-like for the higher ones. These finds are consistent with the theoretical claim of a null current requirement for slope selection, since the pyramidal shape with barely well-defined slopes was observed for the smallest current intensity ($T = 473$ K) while for the largest current intensity ($T = 553$ K), a signature of slope selection is not evident.

The symmetric barrier is the simplest and, for this reason, the most interesting

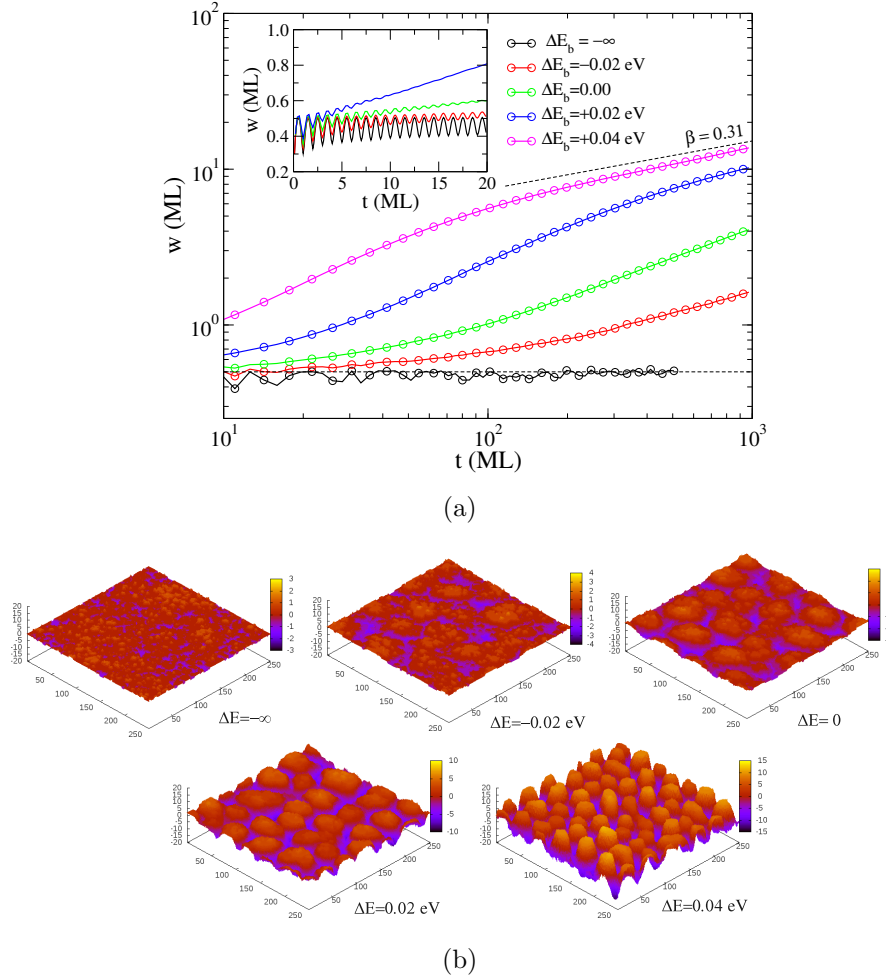


Figure 6. (a) Interface width against time for fixed $T = 573$ K and $E_{b0} = 0.06$ eV and distinct relative step barriers, $\Delta E_b = E_{b0} - E_{bn}$, decreasing from top to bottom. The curves represent averages over 10 independent samples. (b) Surface morphologies after the deposition of 100 ML.

case that produces mound formation. However, we can go beyond this result and investigate the role of other mechanisms by exploring different barriers for bonded and free particles, since there is no restriction imposing equal barriers to both kinds of particles. The interlayer diffusion of bonded particles also plays an essential role for mound formation. In Fig. 6(a), we investigate the relation between step barriers for bonded and free particle by analysing the interface width against time at a growth temperature of $T = 573$ K and a fixed step barrier for free particles $E_{b0} = 0.06$ eV. We define a relative step barrier as $\Delta E_b = E_{b0} - E_{bn}$. When the relative barrier is positive, mounded morphologies with a large interface width are obtained as can be seen in the bottom snapshots of Fig. 6(b). For a negative relative barrier, the surface has a long phase, lasting for several monolayers, with an almost layer-by-layer growth but the kinetic roughening is still observed for sufficiently long times. Videos 3 and 4 of the supplementary material show the surface evolution for negative and positive relative

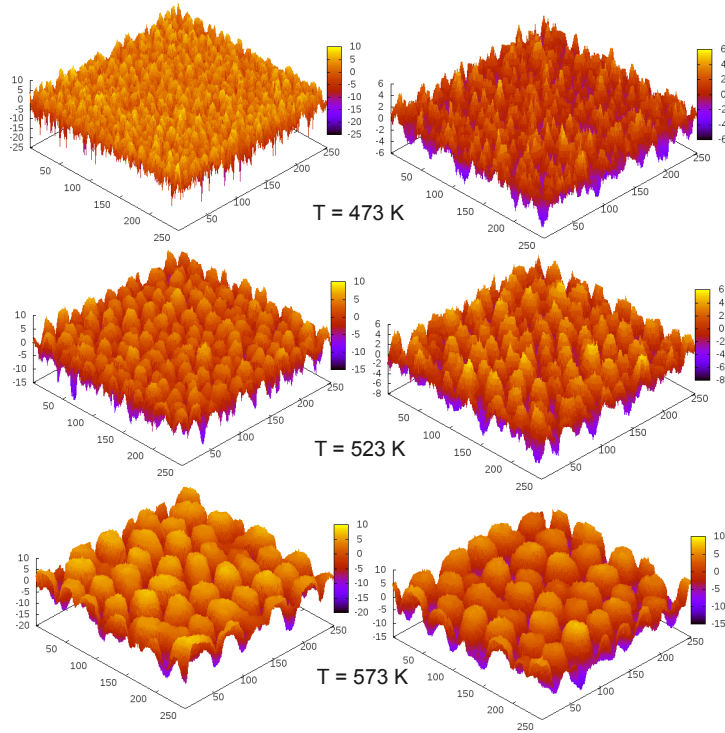


Figure 7. Surfaces at different temperatures obtained after a deposition of 100 ML for the simple SOS (left panels) and WV (right panels) deposition rule.

barriers. The kinetic roughening regime is absent in the extreme case of a forbidden interlayer diffusion of the bonded particles ($E_{bn} = \infty$) as shown in the most top left snapshot of Fig. 6(b) and in Fig. 6(a). Notice that varying the relative step barrier from -0.02 to 0.04 eV, we were able to reproduce a rich variety of spatio-temporal behaviours ranging from layer-by-layer to self-assembled three-dimensional structures. Finally, it is worth noticing that the morphology dynamics does not change considerably for low temperatures when the relative step barrier is varied (data not shown) since, in these cases, the diffusion of bonded particles is itself negligible.

In principle, our model has two competing mechanisms for mound formation: the deposition with a transient mobility and the thermally activated diffusion. However, the transient mobility contribution to mound formation is very weak as shown for the WV model [22] and becomes negligible when compared with the diffusion contribution at temperatures investigated in the present work. However, the transient mobility mechanism is still important to prevent anomalous grooves in surface, particularly, at the lower investigated temperatures. In Fig. 7, we compare surface morphologies generated using a transient mobility deposition rule with simulations using a simple SOS deposition, where the particles are deposited directly in a randomly selected site. Notice that both models generate mounded surfaces even for a small amount of deposited material. As one can see, the surfaces are equivalent at higher temperatures, but at lower temperatures, the surfaces for a simple SOS deposition are featured by grooves that do not correspond to real epitaxial systems. In summary, mound formation is controlled

by the step diffusion rules, but the transient mobility in the deposition works as an important smoothing mechanism at lower temperatures.

5. Conclusions

We have investigated the mound formation in kinetic Monte Carlo simulations of a model for epitaxial film growth with thermally activated diffusion. The model has a step barrier, generically known as Ehrlich-Schwoebel barrier [19, 18], for interlayer diffusion depending on the number of bonds of the adsorbed particle. The step barriers are present for interlayer diffusion when a particle is moving up- or downwardly. Moreover, the rules does not explicitly distinguish between up- and downward diffusion.

Simulations of our bond dependent step barrier (BDSB) model were compared with the standard model having only a downward step barrier (DSB). We have shown that DSB and BDSB are equivalent at low temperatures, when the interlayer diffusion of bonded particles is small. However, if we increase the substrate temperature in a range compatible with several experimental situations (typically $\Delta T \gtrsim 100$ K), the surfaces obtained with the standard model become unrealistic, forming columnar structures with anomalously huge interface widths and step heights. Our model, on other hand, generates well-behaved mounded morphologies, considering a null step barrier for bonded particles. The analysis of the interlayer current shows that DSB has an anomalously large positive (upward) current responsible by the unstable columnar growth, whereas the current in the BDSB model tends to a steady state of balance theoretically required for mound slope selection [15, 16]. When we consider our model with barriers only in descending steps, we observed regular mounded morphology whenever the barrier for bonded particles is smaller than that for free particles. This important result suggests that different barriers for bonded and free particles may be present in real systems.

The case of equal barriers for bonded and free particles in BDSB model was also investigated. This situation is particularly interesting due to the symmetry between down- and upward step barriers (Fig. 1). In odds with previous reports for Wolf-Villain model with an ES barrier in $d = 1 + 1$ dimensions [27], the BDSB model also produces mounds for a symmetric step barrier. A negative interlayer current algebraically approaching a null value (power law decay) was observed, meaning that the balance between down- and uphill diffusion will be reached only at infinite times when the interface widths are already saturated. We have determined the evolution of the interface width and characteristic length in order to characterize the kinetic roughening regimes. The growth and coarsening exponents observed were $\beta \approx 0.31$ and $\zeta \approx 0.22$, respectively. These exponents correspond to the so-called super-roughness scaling regime where $\alpha = \beta/\zeta > 1$.

In the asymmetric case, distinct relative barriers $\Delta E_b = E_{b0} - E_{bn}$ were used. For a negative relative barrier, a long phase with a layer-by-layer growth is observed at early times and a crossover to a kinetic roughening emerges at long times. Nearby this

crossover, a re-entrant dependence of the interface width with temperature is observed. This behaviour was also experimentally observed in the growth of Ag/Ag(100) [30], among other systems [1].

Acknowledgments

This work was partially supported by the Brazilian agencies CNPq and FAPEMIG. SCF thanks the kind hospitality at the Departament de Física i Enginyeria Nuclear/UPC.

References

- [1] Evans J W, Thiel P A and Bartelt M 2006 *Surf. Sci. Rep.* **61** 1–128
- [2] Jorritsma L C, Bijl nagte M, Rosenfeld G and Poelsema B 1997 *Phys. Rev. Lett.* **78** 911–914
- [3] Caspersen K J, Layson A R, Stoldt C R, Fournée V, Thiel P A and Evans J W 2002 *Phys. Rev. B* **65** 193407
- [4] Han Y, Ünal B, Jing D, Qin F, Jenks C J, Liu D J, Thiel P A and Evans J W 2010 *Phys. Rev. B* **81** 115462
- [5] Johnson M D, Orme C, Hunt A W, Graff D, Sudijono J, Sander L M and Orr B G 1994 *Phys. Rev. Lett.* **72** 116–119
- [6] Tadayyon-Eslami T, Kan H C, Calhoun L C and Phaneuf R J 2006 *Phys. Rev. Lett.* **97** 126101
- [7] Zorba S, Shapir Y and Gao Y 2006 *Phys. Rev. B* **74** 245410
- [8] Hlawacek G, Puschig P, Frank P, Winkler A, Ambrosch-Draxl C and Teichert C 2008 *Science* **321** 108–111
- [9] Michely T and Krug J 2003 *Islands, Mounds, and Atoms: Patterns and Processes in Crystal Growth Far from Equilibrium* (Berlin: Springer-Verlag)
- [10] Hamouda A B H, Pimpinelli A and Phaneuf R J 2008 *Surface Science* **602** 2819 – 2827
- [11] Ferreira S O, Bueno I R B, Suela J, Menezes-Sobrinho I L, Ferreira S C and Alves S G 2006 *Appl. Phys. Lett.* **88** 244102
- [12] Shim Y, Borovikov V and Amar J G 2008 *Phys. Rev. B* **77** 235423
- [13] Ramasco J J, López J M and Rodríguez M A 2000 *Phys. Rev. Lett.* **84** 2199–2202
- [14] Šmilauer P and Vvedensky D D 1995 *Phys. Rev. B* **52** 14263–14272
- [15] Siegert M and Plischke M 1994 *Phys. Rev. Lett.* **73** 1517–1520
- [16] Schinzer S, Köhler S and Reents G 2000 *Eur. Phys. J. B* **15** 161–168
- [17] López J M, Rodríguez M A and Cuerno R 1997 *Phys. Rev. E* **56** 3993–3998
- [18] Schwoebel R L and Shipsey E J 1966 *J. Appl. Phys.* **37** 3682–3686
- [19] Ehrlich G and Hudda F G 1966 *J. Chem. Phys.* **44** 1039–1049
- [20] Amar J G and Family F 1996 *Phys. Rev. Lett.* **77** 4584–4587
- [21] Murty M R and Cooper B 2003 *Surf. Sci.* **539** 91–98
- [22] Chatrathorn P P, Toroczkai Z and Das Sarma S 2001 *Phys. Rev. B* **64** 205407
- [23] Pierre-Louis O, D’Orsogna M R and Einstein T L 1999 *Phys. Rev. Lett.* **82** 3661–3664
- [24] Clarke S and Vvedensky D D 1987 *Phys. Rev. Lett.* **58** 2235–2238
- [25] Clarke S and Vvedensky D D 1988 *J. Appl. Phys.* **63** 2272–2283
- [26] Leal F F, Ferreira S C and Ferreira S O 2011 *J. Phys.: Condens. Matter* **23** 292201
- [27] Rangdee R and Chatrathorn P 2006 *Surf. Sci.* **600** 914 – 920
- [28] Wolf D E and Villain J 1990 *Eur. Lett.* **13** 389
- [29] J Villain 1991 *J. Phys. I France* **1** 19–42
- [30] Stoldt C R, Caspersen K J, Bartelt M C, Jenks C J, Evans J W and Thiel P A 2000 *Phys. Rev. Lett.* **85** 800–803
- [31] Bartelt M C and Evans J W 1999 *Surface Science* **423** 189–207

- [32] Shim Y and Amar J G 2010 *Phys. Rev. B* **81** 045416